

Making the most of Taylor expansion and imaginary μ

E. Laermann, F. Meyer

Fakultät für Physik, Universität Bielefeld, D-33615 Bielefeld, Germany

M. P. Lombardo

INFN-Laboratori Nazionali di Frascati, I-00044, Frascati (RM) Italy

Abstract. We present preliminary results for the curvature of the pseudocritical line and susceptibilities in $N_f = 2 + 1$ flavor QCD. The computations are carried out on lattice sizes of $16^3 \times 4$, at matching parameters of early work of the Bielefeld group. Emphasis is placed on the control of systematic errors, by cross-validating results obtained by use of the Taylor expansion and measurements at imaginary chemical potential. To this end, we generalize the magnetic equation of state to the analysis of the number density, and we extend it to imaginary values of the chemical potential.

1. Introduction

Most likely, a large fraction of the participants in this meeting are familiar with the challenges faced by lattice QCD at non-zero baryon density [1]: the region of quark chemical potential μ_q exceeding $m_\pi/2$ remains prohibitively difficult, due to a severe sign problem [2].

For smaller chemical potential a variety of methods have been proposed to circumvent these difficulties, which have been quite successful in many respects. However, even in the easy region $\mu_q < m_\pi/2$ there are challenges to face: for instance, it has been noted that most current estimates of the QCD endpoint lie dangerously close to the 'forbidden region' $\mu_q > m_\pi/2$; the qualitative agreement among different results on the slope of the critical line still needs to be corroborated by some convincing continuum estimates obtained with different methods. And, there is a growing interest in the values of higher order susceptibilities, particularly at larger values of the chemical potential, while the current results are limited to the lowest order ones [3]. So there is room for improvement, which can perhaps be achieved by mixing and matching different approaches.

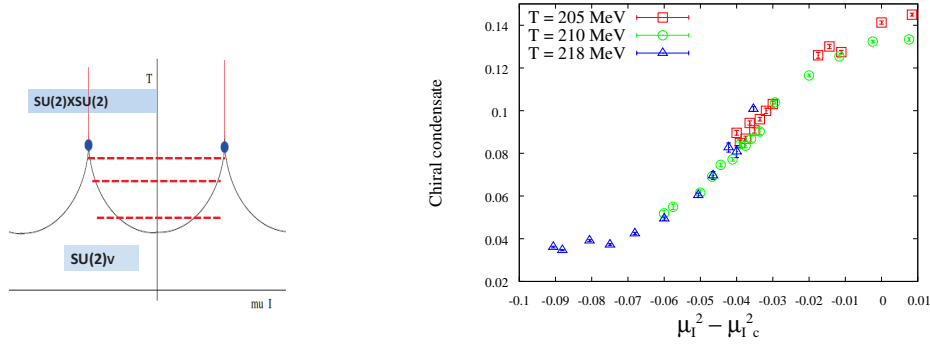


Figure 1. A sketchy view of the phase diagram of QCD for two massless flavors in the temperature, imaginary chemical potential plane, with the superimposed trajectories of our simulations. The blue points indicate the Roberge-Weiss endpoint (left). The chiral condensate measured along such trajectories, plotted against the rescaled chemical potential $\mu^2 - \mu_c^2(T)$ (right). Note the (approximate) universal behaviour of the condensate.

2. Two complementary approaches: Taylor expansion and imaginary chemical potential

One way to handle the physics of small chemical potential relies on Taylor expansion [4]. This approach is well understood mathematically, however it only works inside its convergence circle, whose radius is unknown. Moreover even inside the circle it is hard to judge when convergence has been achieved. Alternatively, analytic continuation from imaginary chemical potential – where conventional simulations are possible – to real chemical potential can in principle be extended to the entire analytic domain, but the danger here is a possible lack of control over the continuation itself: for instance, terms which are subleading for imaginary chemical potential might well become leading for real chemical potential. The strengths of the two methods are somewhat complementary, and their weaknesses different: this suggests to develop a hybrid method which combines the two, and this note reports on our ongoing effort in this direction [5].

3. Results

Our study for staggered 2+1 flavors on lattices of size $16^3 \times 4$ clearly is exploratory. However, the quark mass values are close to the ones realized in nature. The Goldstone pion mass is tuned to about 220 MeV and the kaon acquires its physical mass. This corresponds to a (degenerate) light to strange quark mass ratio of $m_l/m_s = 1/10$. The action utilized is the p4fat3 action for which Taylor coefficients computed at $\mu = 0$ are available in our range of temperatures and at our quark masses [4]. The computations were carried out at three temperatures above the critical temperature for two massless flavors for the considered lattice spacings: $T = 205, 210, 218$ MeV. In Fig.1, left we sketch the simulations' trajectories, alongside the critical line in the chiral limit, in the μ_I, T plane. The sketch evidences the μ_I periodicity as well as the symmetry under reflection $\mu_I \rightarrow -\mu_I$; the actual simulations were performed only at positive three-flavor degenerate μ_I , and within the first half-period. The blue points mark the endpoint of the Roberge Weiss phase transition. The light quark chiral condensate, plotted in Fig.1, right, is showing a fairly rapid rise

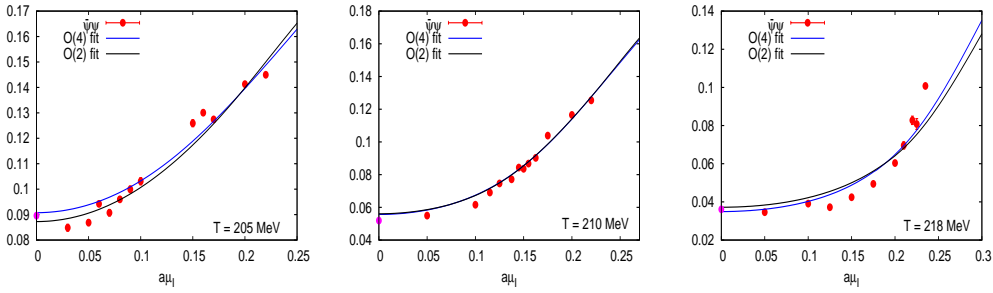


Figure 2. The fits motivated by the magnetic Equation of State for the chiral condensate, superimposed to the data point.

when μ_I is increased, signaling the pseudocritical point for the transition to the broken phase (marked $SU(2)_V$ in the diagram). We plot the results against a rescaled chemical potential to confirm the feasibility of a scaling study based on the magnetic Equation of State.

3.1. The magnetic Equation of State

Consider now the magnetic equation of state

$$M = h^{1/\delta} f_G(z) \quad z = th^{\frac{-1}{\beta\delta}} \quad (1)$$

where M and h are identified with the light chiral condensate and the light bare mass: $M = m_s \langle \bar{\psi}\psi \rangle_l$, $h = \frac{1}{h_0} \frac{m_l}{m_s}$ respectively, f_G is a scaling function which only depends on the universality class of the transition, and $t = 0$ defines the critical line. Our light mass does not change: if scaling (i.e. Eq. 1) holds true the chiral condensate results plotted versus $\mu^2 - \mu_c^2(T)$, where $\mu_c^2(T)$ is the critical chemical potential for each temperature T , should fall on a single curve. In Fig.1 we see that this is indeed happening, demonstrating the universal behaviour of the chiral condensate at least in the range of parameters we are exploring. $\mu_c^2(T)$ is found by searching for the optimal match between results for different temperatures, and compares favorably with alternative estimates.

3.2. Curvature of the critical line from the magnetic EoS

For small chemical potential t can be explicitly written as

$$t = \frac{1}{t_0} \left(\frac{T - T_c}{T_c} + k(\mu/T)^2 \right) \quad (2)$$

where T_c is the critical temperature in the chiral limit. The standard condition $f_G(0) = f'_G(0) = 1$ fixes the normalization t_0 and h_0 which have been determined in Ref. [6]. As a working hypothesis we assume that t_0 and h_0 do not depend on the temperature, and we check a posteriori that this indeed is the case. k – the curvature of the critical line – can then be computed from the Equation of State, using the explicit forms available for the two plausible universality classes $O(2)$ and $O(4)$, and the results contrasted with those obtained in Ref. [7].

From the EoS for the order parameter one can derive analogous relations for the magnetic susceptibility, as well as for the number density n and its susceptibility [8], leading to alternative estimates of k . To fix the notation, let

Table 1. The results for the curvature of the critical line k (Eq.(2)) from the fits to the magnetic EoS for the chiral condensate ($k_{\bar{\psi}\psi}$), and from the fits to the number density (k_n).

T(MeV)	$k_{\bar{\psi}\psi}$			k_n		
	205	210	218	205	210	218
O(2)	0.026(1)	0.031(1)	0.025(3)	0.021(1)	0.021(1)	0.016(1)
O(4)	0.022(1)	0.028(1)	0.025(3)	0.039(1)	0.036(1)	0.023(2)

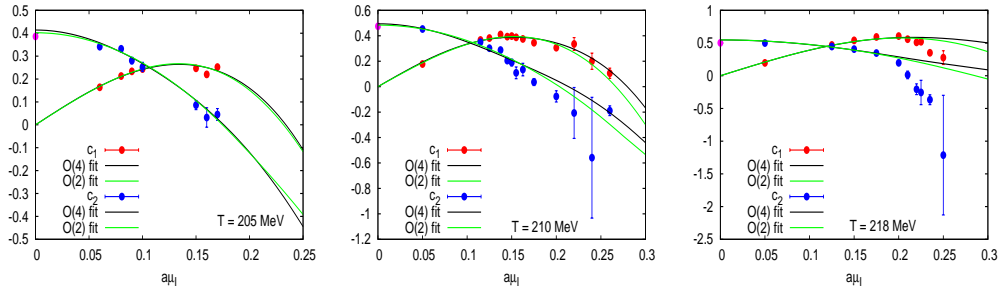


Figure 3. The fits motivated by the magnetic Equation of State for c_1 and c_2 (related to quark number and its susceptibility respectively, see text) superimposed to the data points.

us write the Taylor expansion of the pressure in terms of the quark chemical potentials around a generic $\mu_0 = (\mu_{u,0}, \mu_{d,0}, \mu_{s,0})$ for our $N_f = 2 + 1$ system:

$$\frac{p}{T^4}(\hat{\mu}) = \sum_{k,l,n} c_{kl n} (\hat{\mu}_u - \hat{\mu}_{u,0})^k (\hat{\mu}_d - \hat{\mu}_{d,0})^l (\hat{\mu}_s - \hat{\mu}_{s,0})^n$$

with the abbreviation $\hat{\mu}_q = \mu_q/T$ and the coefficients

$$c_{kl n} = \frac{1}{k!l!n!} \frac{\partial^k}{\partial \hat{\mu}_u^k} \frac{\partial^l}{\partial \hat{\mu}_d^l} \frac{\partial^n}{\partial \hat{\mu}_s^n} \left(\frac{p}{T^4} \right) \quad (3)$$

evaluated at μ_0 . We will in particular discuss $c_1 = c_{100}$ and $c_2 = c_{200}$, which are related to the particle number and its susceptibility. In Fig.2 and Fig.3 we show the results of the EoS fits and in Table 1 we record the k values returned by the fits for the chiral condensate and the quark number (the coefficient c_1). While the fit results, at least for O(2), do not seem to be inconsistent, it is clear that at values for μ_I close to the Roberge-Weiss limit other scaling studies need to be performed, work for the future.

3.3. The Taylor expansion

How far in μ we can trust the Taylor expansion? A direct comparison of the number density of e.g. the u quark given by the partial sums of its Taylor series:

$$\frac{n_u}{T^3}(\hat{\mu}) = \sum_{k,l,n} k c_{kl n} (\hat{\mu}_u - \hat{\mu}_{u,0})^{k-1} (\hat{\mu}_d - \hat{\mu}_{d,0})^l (\hat{\mu}_s - \hat{\mu}_{s,0})^n. \quad (4)$$

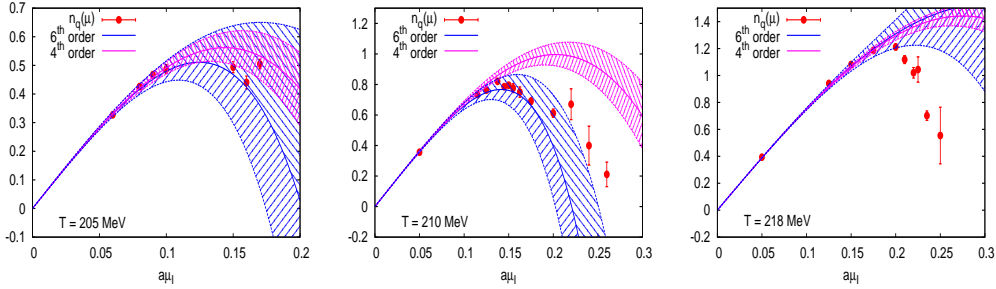


Figure 4. The results for the number density at imaginary chemical potential, contrasted with the partial sums of the Taylor series of the indicated order.

with results obtained directly at imaginary μ might give the answer. We show the results for increasing temperatures in Fig.4: for $T = 205$ MeV a good convergence is achieved indicating a small contribution from the 8^{th} order terms and superior ones. At the highest temperature instead the results suggest that a 6^{th} order expansion is not capable to describe the data at $\mu_I \approx 0.2$. The simultaneous consideration of Taylor expansion and imaginary μ results naturally suggests a strategy to extract higher order terms of the expansions – or, equivalently, higher order susceptibilities – without having to implement the cumbersome higher order derivatives. At the same time one can place lower bounds on the radius of convergence simply by assessing by eye the extent of the region where actual convergence is achieved.

4. Parting comments

We have presented an overview of results obtained by performing simulations at zero and non-zero imaginary chemical potential. We have noted that an analysis based on the magnetic equation of state for the chiral condensate, the number density and their susceptibilities at imaginary chemical potential gives information on the universality class of the transition for two massless flavors, and on the slope of the chiral line. We have argued that the simultaneous consideration of results from the Taylor expansion at $\mu = 0$ and at imaginary μ can place a lower bound on the radius of convergence at $\mu = 0$, and facilitate the computation of higher order coefficients.

References

- [1] G. Aarts, PoS LATTICE **2012** 017 (2012).
- [2] K. Splitteroff, PoS LATTICE **2006**, 023 (2006).
- [3] M. P. Lombardo, PoS LATTICE **2012**, 016 (2012).
- [4] M. Cheng et al., Phys. Rev. D79 (2009) 074505.
- [5] F. Meyer, Master thesis, Bielefeld 2012.
- [6] S. Ejiri et al., Phys. Rev. D80 (2009) 094505.
- [7] O. Kaczmarek et al., Phys. Rev. D83 (2011) 014504.
- [8] J. Engels and F. Karsch, Phys. Rev. D85 (2012) 094506.